Higgs searches with ATLAS

Mathieu Aurousseau, on behalf of the ATLAS collaboration
University of Johannesburg, Johannesburg, South Africa
E-mail: mathieu.aurousseau@cern.ch

Abstract. This document is an overview of the recent results from the ATLAS experiment at the Large Hadron Collider (LHC) in the search for a Standard Model Higgs boson, using an integrated luminosity of 4.8 fb^{-1} and 13 fb^{-1} of data at a center-of-mass energy of 7 TeV or 8 TeV, respectively. Results are presented for the $H \to ZZ^{(*)} \to 4\ell$, $H \to \gamma\gamma$, $H \to WW^{(*)} \to e\nu\mu\nu$, $H \to \tau\tau$ and $H \to b\bar{b}$ search channels. An update on the combination of the various channels and on the measurement of the properties (spin, parity) of the observed state is given.

ATL-PHYS-PROC-2013-098
30 April 2013

1. Introduction

In July 2012, the ATLAS [1] and CMS [2] collaborations reported the observation of a new particle in the search for a Standard Model (SM) Higgs boson [3, 4], using the data collected until June 2012. In both cases, the claim was made using a combination of several sensitive channels, but no observation was claimed in individual channels. In this paper, the results published at the time of the ECTP2013 conference by the ATLAS collaboration are presented. These correspond to an integrated luminosity of 4.8 fb^{-1} and 13 fb^{-1} of data from the Large Hadron Collider (LHC) at center-of-mass energies of 7 TeVand 8 TeV, respectively. The individual channels described in this note are: $H \to ZZ^{(*)} \to 4\ell$, $H \to \gamma\gamma$, $H \to WW^{(*)} \to e\nu\mu\nu$, $H \to \tau\tau$ and $H \to b\bar{b}$. The combination and measurements of the mass, spin and parity are also presented. If the first three channels are the most sensitive ones, the last two are of crucial importance to assess and measure the couplings of the Higgs boson to fermions.

2. $H \to ZZ^{(*)} \to 4\ell$

The $H \to ZZ^{(*)} \to 4\ell$ channel [5] is often considered as the "golden channel" and is characterized by a large signal-to-background ratio, and a high mass resolution. However, only a small number of events is expected in this channel. The current analysis uses the $\sqrt{s} = 7$ TeV and $\sqrt{s} = 8$ TeV datasets, corresponding to integrated luminosities of 4.6 fb^{-1} and 13 fb^{-1} respectively. The experimental signature is based on the selection of well-identified isolated leptons forming two same-flavor, opposite sign pairs. The four leptons are required to pass kinematic cuts, in particular $p_T > 20, 15, 10$ and 7 (6) GeV for electrons (muons). The lepton pair with an invariant mass closest to the Z boson mass is called the primary pair, and is required to have a mass between 50 GeV $< m_{12} <$ 106 GeV. The mass requirement on the other (secondary) pair is relaxed and depends on the total 4-lepton mass ($m_{4\ell}$). At $m_{4\ell} = 125$ GeV, the secondary pair is required to have a mass between 17.5 GeV $< m_{34} <$ 115 GeV.

The irreducible background to this channel is the direct production of $ZZ^{(*)}$ events. The shape and normalization are estimated using Monte Carlo and theoretical predictions. The main

	Signal ($m_H = 125$GeV)	$ZZ^{(*)}$	$Z+$jets, $t\bar{t}$	Observed
4μ	4.0 ± 0.5	2.03 ± 0.09	0.36 ± 0.09	8
$2\mu 2e$	1.7 ± 0.2	0.70 ± 0.05	1.21 ± 0.18	2
$2e2\mu$	2.4 ± 0.3	1.02 ± 0.05	0.30 ± 0.07	4
$4e$	1.8 ± 0.3	0.94 ± 0.09	1.72 ± 0.23	4
Total	9.9 ± 1.3	4.7 ± 0.3	3.6 ± 0.3	18

Table 1. Number of expected and observed events in each final state category in the window $120 < m_{4\ell} < 130$ GeV, for the combined $\sqrt{s} = 7$ TeV and $\sqrt{s} = 8$ TeV datasets [5].

reducible backgrounds are $Z+$jets and $t\bar{t}$, estimated from data-driven methods. The dominant background depends on the flavor of the secondary leptons: in the case of muons, the dominant background is the irreducible $ZZ^{(*)}$, while in the case of electrons, the reducible background dominates. The number of expected and observed events in each category is summarized in Table 1.

The number of observed events is in good agreement with the combined number of signal and backgrounds events, while there is an excess with respect to the background-only hypothesis. This is also visible in the 4ℓ-mass spectrum shown in Fig. 1 (left). The excess is characterized by the probability, p_0, that the background-only hypothesis is more signal-like than the observed data. For the combined dataset, the observed local p_0 is $2.1 \cdot 10^{-5}$, which corresponds to 4.1σ (3.1σ expected), as shown on Fig. 1 (right). The signal strength (ratio between the measured and expected cross-sections) is $\mu = 1.3^{+0.5}_{-0.4}$, which is in agreement with the SM ($\mu = 1$).

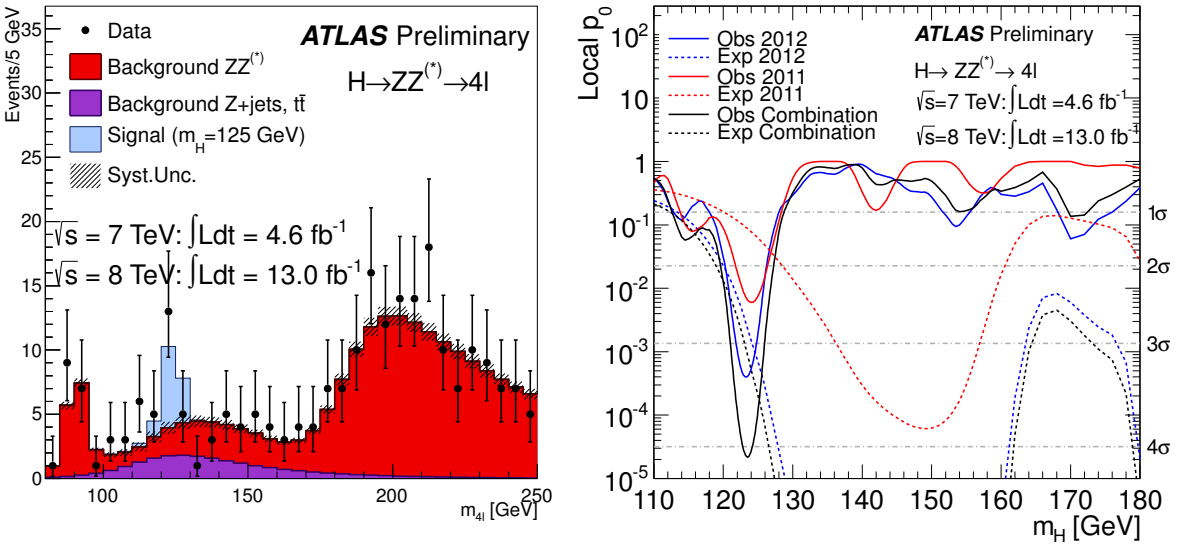

Figure 1. The 4ℓ invariant mass spectrum (left) and the observed local p_0 (right) in the $H \to ZZ^{(*)} \to 4\ell$ channel, using the combined dataset [5].

3. $H \to \gamma\gamma$

The $H \to \gamma\gamma$ channel [6] is also a high-mass-resolution channel, but unlike the $H \to ZZ^{(*)} \to 4\ell$ case, a large number of events is expected with the analyzed dataset. The presented analysis

uses the $\sqrt{s} = 7$ TeV and $\sqrt{s} = 8$ TeV datasets, corresponding to integrated luminosities of 4.8 fb^{-1} and 13 fb^{-1} respectively. The event selection is based on two well-identified, isolated, high transverse momentum photons ($E_T > 40, 30$ GeV). This channel is characterized by the presence of large irreducible ($\gamma - \gamma$) and reducible (γ-jet, jet-jet) backgrounds. The expected signal-to-background ratio is of the order of a few percent for the inclusive selection. The sensitivity of the channel is optimized by the definition of 12 exclusive categories, each having a different signal-to-background ratio and mass resolution. Nine categories are based on the kinematics (centrality, transverse momentum) and topology (presence of converted photons) of the events, while the remaining three depend on the production process (one for the vector boson fusion (VBF), two for the associated production with a vector boson). The last two categories are applied only on the $\sqrt{s} = 8$ TeV dataset.

As shown on Fig. 2 (left), an excess is seen above the background, and this excess is characterized by the local p_0 shown on Fig. 2 (right). For the combined dataset, the observed local p_0 is $4.4 \cdot 10^{-10}$, which corresponds to 6.1σ (3.3σ expected). This means that a discovery can be claimed in the $H \to \gamma\gamma$ channel alone. The signal strength is $\mu = 1.80^{+0.48}_{-0.36}$, corresponding to a 2.2σ deviation from the SM hypothesis.

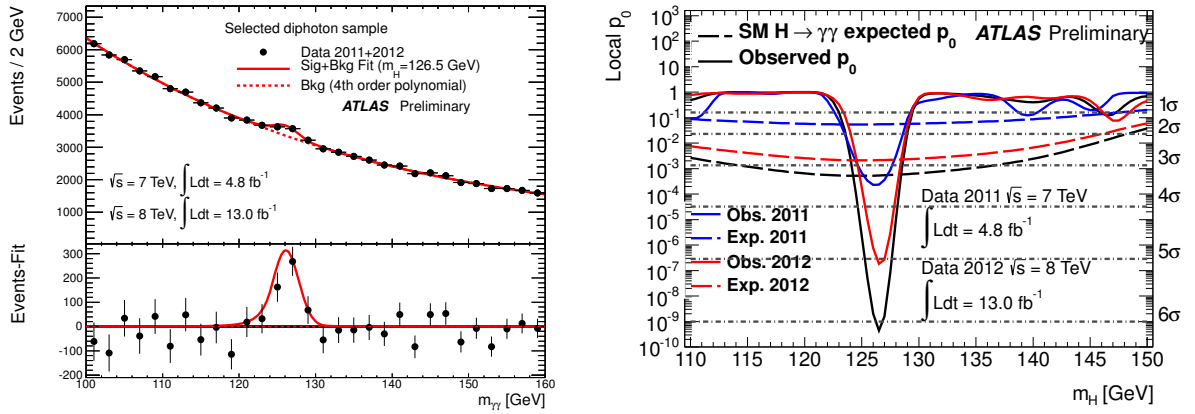

Figure 2. The $\gamma\gamma$ invariant mass spectrum (left) and the observed local p_0 (right) in the $H \to \gamma\gamma$ channel, using the combined dataset [6].

4. $H \to WW^{(*)} \to e\nu\mu\nu$

In the $H \to WW^{(*)}$ channel [7], the expected signal-to-background ratio is about 10%. This channel has the largest branching fraction for a Higgs boson mass above 130 GeV. Due to the presence of neutrinos in the final state, the discriminating variable is the transverse mass m_T, which includes the transverse kinematics from the leptons as well as the missing transverse momentum. This channel is most sensitive for mixed flavor final states, i.e. $H \to WW^{(*)} \to e\nu\mu\nu$, which suffers little from the Drell-Yan (dilepton) background. The presented search is performed using the $\sqrt{s} = 8$ TeV dataset only, corresponding to an integrated luminosity of 13 fb^{-1}. Events with two well-identified, high-momentum leptons ($p_T > 25, 15$ GeV) are selected. The Drell-Yan, Z + jets and $t\bar{t}$ reducible backgrounds are rejected using cuts on the missing transverse energy and the transverse mass. Direct $WW^{(*)}$ production is rejected using spin correlation (the leptons tend to be in produced in the same direction in the case if $H \to WW^{(*)} \to e\nu\mu\nu$ events). In particular, the dilepton transverse invariant mass $m_{\ell\ell}$ is required to be lower than 50 GeV, and the azimuthal angle between the leptons $\Delta\phi_{\ell\ell}$ to be less than 1.8.

	Signal ($m_H = 125$GeV)	$WW^{(*)}$	top	others	Total background	Observed
$H + 0$ jet s	45 ± 9	242	27	64	334 ± 28	423
$H + 1$ jet	18 ± 6	40	50	23	114 ± 18	141

Table 2. Number of expected and observed events in each final state category for $m_H = 125$ GeV in the window $0.75m_H < m_T < m_H$ [7].

Categories are then defined depending on the number of jets and the flavor of the leading (highest transverse momentum) lepton. Events with 0 jet are dominated by the $WW^{(*)}$ background, while those with 1 jet are dominated by top backgrounds. The number of expected signal ($m_H = 125$ GeV) and background events, as well as the number of observed events, are shown in Table 2.

The number of observed events is in good agreement with the combined number of signal and backgrounds events, while there is an excess with respect to the background-only hypothesis. This excess can also be seen on Fig. 3 (left), which shows the transverse mass spectrum after subtraction of the expected background. Figure 3 (right) shows the local p_0 after combination of the search categories. The observed local p_0 is $4 \cdot 10^{-3}$, which corresponds to 2.6σ (1.9σ expected). The signal strength is $\mu = 1.5 \pm 0.6$, which is in agreement with the SM hypothesis.

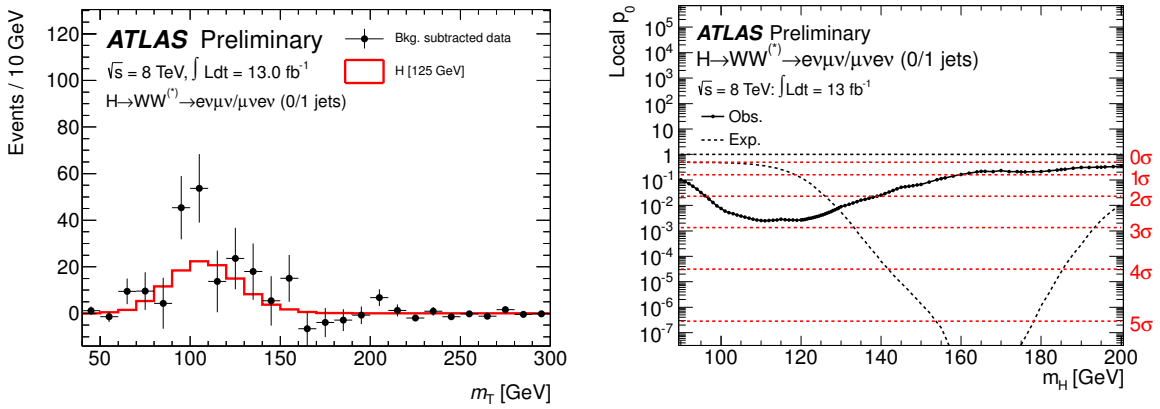

Figure 3. The transverse mass (m_T) spectrum with the predicted signal for $m_H = 125$ GeV (left) and the observed local p_0 (right) in the $H \to WW^{(*)} \to e\nu\mu\nu$ channel [7].

5. $H \to \tau\tau$

The $H \to \tau\tau$ channel [8] is characterized by a large branching fraction around $m_H = 125$ GeV and a large $Z \to \tau\tau$ background. The current analysis uses the $\sqrt{s} = 7$ TeV and $\sqrt{s} = 8$ TeV datasets, corresponding to integrated luminosities of 4.8 fb^{-1} and 13 fb^{-1} respectively. In order to optimize the sensitivity of this channel, the events are divided into 25 categories depending on the nature of the τ decay (two leptonic, one leptonic and one hadronic, two hadronic), the number of jets, the production mode (vector boson fusion and associated production). Boosted categories (high-momentum $\tau\tau$ system) are also added to benefit from a better rejection between $Z \to \tau\tau$ and $H \to \tau\tau$ events. The event selection is based on the reconstruction of τ leptons using a Boosted Decision Tree (BDT). The main backgrounds come from $Z \to \tau\tau$ events, as well as top and multijets events. The discriminating variable is the $\tau\tau$ invariant mass.

In this channel, only a modest excess of events above the background-only hypothesis is observed, and an exclusion limit at the 95% CL is drawn, as shown on Fig. 4 (left). At $m_H = 125$ GeV, the observed limit is 1.9 times the SM cross-section (1.2 expected). Figure 4 (right) shows the local p_0 after combination of the analysis categories. The observed local p_0 is $1.3 \cdot 10^{-1}$, which corresponds to 1.1σ (1.7σ expected), and the signal strength is $\mu = 0.7 \pm 0.7$, meaning that the observation is compatible with both the SM and background-only hypotheses.

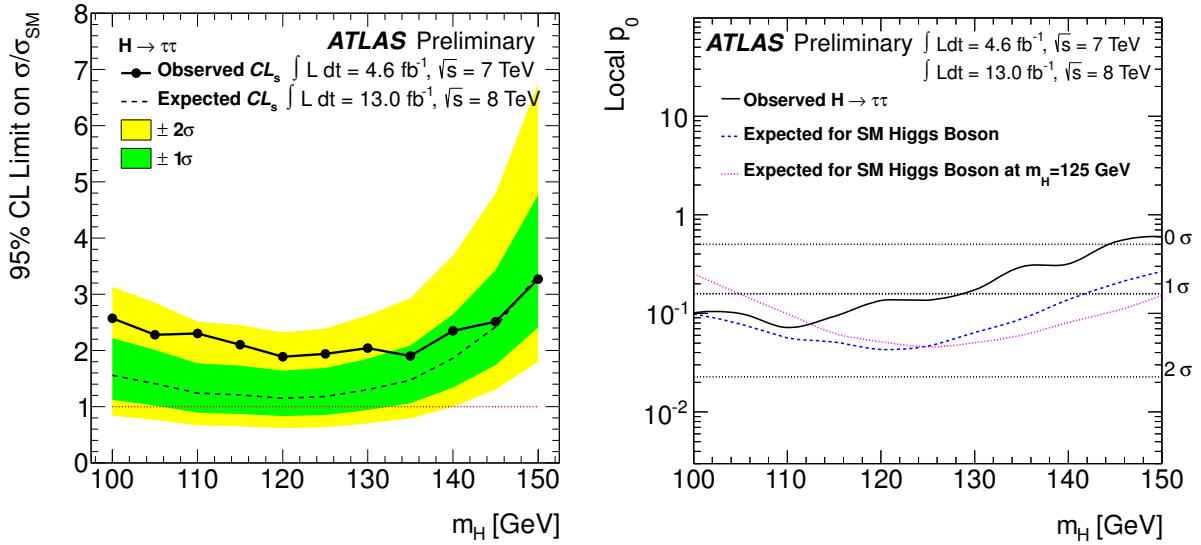

Figure 4. Observed (solid) and expected (dashed) 95% confidence level upper limits on the Higgs boson cross-section times branching ratio, normalised to the SM expectation, as a function of the Higgs boson mass (left), and the observed local p_0 (right) in the $H \to \tau\tau$ channel. Both plots include all analysis categories for the combined $\sqrt{s} = 7$ TeV and $\sqrt{s} = 8$ TeV datasets [8].

6. $H \to b\bar{b}$

The $H \to b\bar{b}$ channel [9] has the largest branching fraction for $m_H = 125$ GeV, but suffers from a very large QCD background. Only the production in association with a gauge boson (W, Z) is considered. The selection is based on the reconstruction of 2 b-jets identified with a b-tagging algorithm, with a transverse momentum larger than 45 and 25 GeV respectively. Three categories depending on the gauge boson decay are defined:

- 2 leptons, low missing transverse momentum and dilepton invariant mass compatible with the Z boson mass: events produced in the ZH mode, where the Z boson decays to 2 leptons;
- 1 lepton, large transverse momentum and transverse mass compatible with the W boson mass: events produced in the WH mode, where the W boson decays to 1 lepton and 1 neutrino; and
- 0 lepton and large transverse momentum: events produced in the ZH mode, where the Z boson decays to 2 neutrinos.

The events are then divided into more categories depending on the number of additional jets, amount of missing transverse momentum, and the momentum of the gauge boson, leading to a total of 16 categories. Analysis cuts are optimized in each category to achieve the best possible sensitivity.

The main backgrounds come from diboson events (shape and normalization taken from simulation), QCD multijet events (data-driven estimation), top and W/Z+jets (shape from simulation and normalization from control regions).

In this channel, no excess of events is seen above the background-only hypothesis, and an exclusion limit at the 95% CL is drawn, as shown on Fig. 5 (left). At $m_H = 125$ GeV, the observed limit is 1.8 times the SM cross-section (1.9 expected). Figure 5 (right) shows the local p_0 after combination of the analysis categories. The observed local p_0 is 0.64 (0.15 expected), and the signal strength is $\mu = -0.4 \pm 0.7(\text{stat.}) \pm 0.8(\text{syst.})$, meaning that the observation is compatible with the background-only hypotheses.

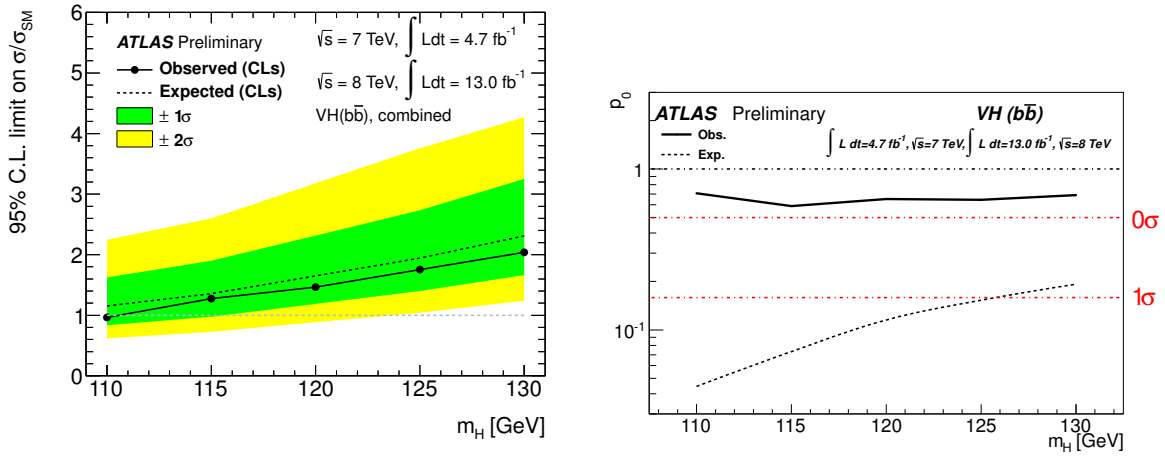

Figure 5. Observed (solid) and expected (dashed) 95% confidence level upper limits on the Higgs boson cross-section times branching ratio, normalised to the SM expectation, as a function of the Higgs boson mass (left), and the observed local p_0 (right) in the $H \to b\bar{b}$ channel. Both plots include all analysis categories for the combined $\sqrt{s} = 7$ TeV and $\sqrt{s} = 8$ TeV datasets [9].

7. Combination of all channels

The combination of all channels presented above [10] leads to an observed local p_0 of 10^{-12}, which corresponds to a significance of 7σ. The measured signal strength, shown on Fig. 6 (left) is $\mu = 1.35 \pm 0.19(\text{stat.}) \pm 0.15(\text{syst.})$, which is compatible with the SM expectation ($\mu = 1$). The mass is extracted from the two high-mass-resolution channels, namely $H \to ZZ^{(*)} \to 4\ell$ and $H \to \gamma\gamma$, which give respectively: $123.5 \pm 0.8(\text{stat.}) \pm 0.3(\text{syst.})$ GeV and $126.6 \pm 0.3(\text{stat.}) \pm 0.7(\text{syst.})$ GeV. The combined mass, shown on Fig. 6 (right), is $125.2 \pm 0.3(\text{stat.}) \pm 0.6(\text{syst.})$ GeV. The discrepancy between the two individual channels corresponds to between 2.3 and 2.7 standard deviation, depending on how the systematic uncertainties are taken into account.

8. Measurement of spin and parity

Besides the mass and signal strength, the properties (spin, parity) of the observed new boson have to be measured in order to assess if it is indeed the scalar boson predicted by the SM. The spin 1 hypothesis is strongly disfavored by the observation of $H \to \gamma\gamma$ events. The spin 2 hypothesis is compatible with the bosonic decays observed ($H \to ZZ^{(*)}$, $H \to \gamma\gamma$, $H \to WW^{(*)}$), but would be excluded by a clear observation of fermionic decays ($H \to \tau\tau$, $H \to b\bar{b}$).

The parity is also an interesting property to measure, since its prediction differs depending on the models: the SM predicts a 0^+ state while some supersymmetric models predict a 0^- state.

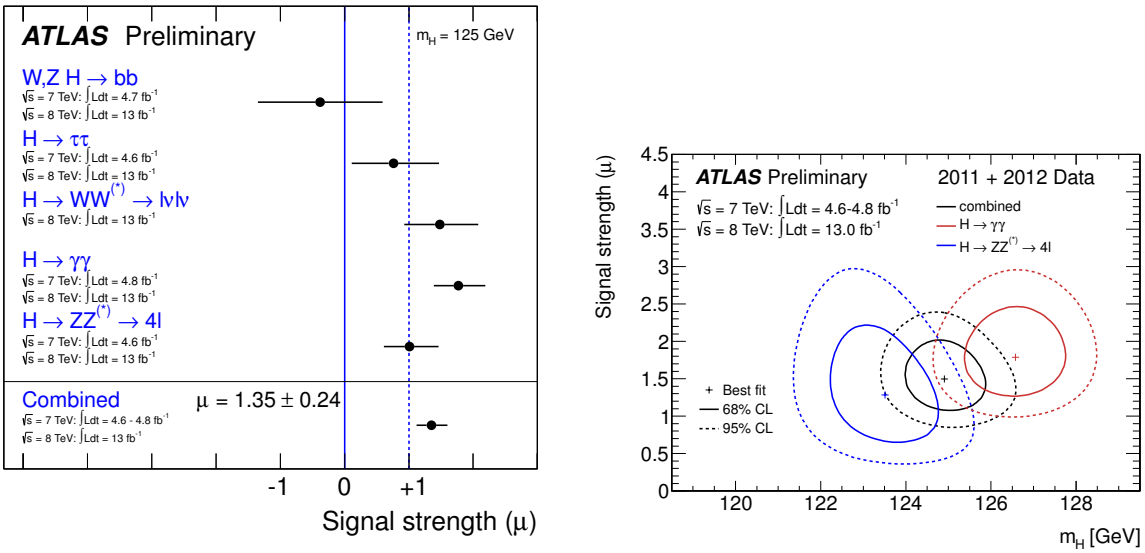

Figure 6. Combined measurement of the signal strength from all channels (left) and of the new particle mass from the sensitive channels $H \to ZZ^{(*)} \to 4\ell$ and $H \to \gamma\gamma$ (right) [10].

Other models are also tested here: spin 2^+ (graviton-like) and 2^- (pseudo-tensor). Studies of the spin and parity properties of the candidate Higgs boson, using angular variables in the $H \to \gamma\gamma$ [6] and the $H \to ZZ^{(*)} \to 4\ell$ [5] channels, are presented below.

8.1. Spin and parity from $H \to \gamma\gamma$ events

Using $H \to \gamma\gamma$ events, the 0^+ and 2^+ hypotheses are tested. The distribution used is $|\cos\theta^*|$, where θ^* is the angle between the two photons in the Collins-Sopper frame. This distribution is expected to be flat (before acceptance cuts) for a spin 0 particle but not for a spin 2 particle. Figure 7 (left) shows the background-subtracted $|\cos\theta^*|$ distribution for the two spin hypotheses and for data. Only events in the $\sqrt{s} = 8$ TeV dataset and in the signal region (between 123.8 and 128.6 GeV) are considered. The compatibility of the observed events with the two spin hypotheses is assessed with a likelihood ratio, as shown on Fig. 7 (right). The two distributions are expected to be well-separated (1.8σ). The spin 2^+ hypothesis is excluded at the 91% CL while the observation is compatible with the spin 0^+ hypothesis (SM) within 0.5σ.

8.2. Spin and parity from $H \to ZZ^{(*)} \to 4\ell$ events

With $H \to ZZ^{(*)} \to 4\ell$ events, the $0^\pm$ and $2^\pm$ hypotheses are tested, using 5 angular distributions. Two methods are applied: one using a BDT and one using a matrix element based likelihood ratio (J^p-MELA, more details can be found in [5]). Both give compatible results. Only events in the signal region between 115 and 130 GeV are considered. The compatibility of the observed events with two spin hypotheses is assessed with a likelihood ratio, as shown on Fig. 8 (left) for 0^+ and 0^-, and on Fig. 8 (right) for 0^+ and 2^+.

When comparing to the SM hypothesis (0^+), the 0^- hypothesis is excluded at the 99% CL (96% expected) and the 2^+ hypothesis is excluded at the 85% CL (80% expected). The data are compatible with the 0^+ hypothesis within 0.18σ.

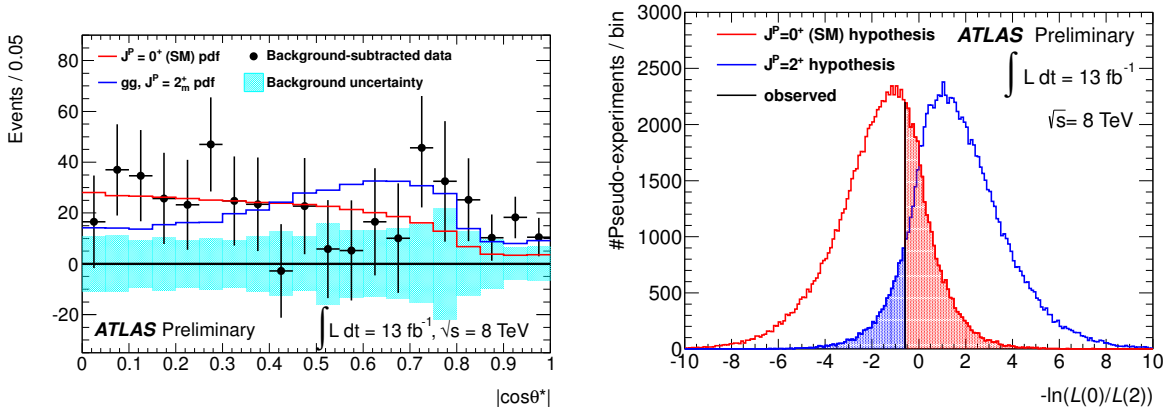

Figure 7. Distribution of $|\cos\theta^*|$ after subtraction of background for $H \to \gamma\gamma$ events in the signal region, for the $\sqrt{s} = 8$ TeV dataset only (left), and the distribution of the likelihood ratio in 100k pseudo-experiments for the spin 0 (red) and spin 2 (blue) hypotheses (right) [6].

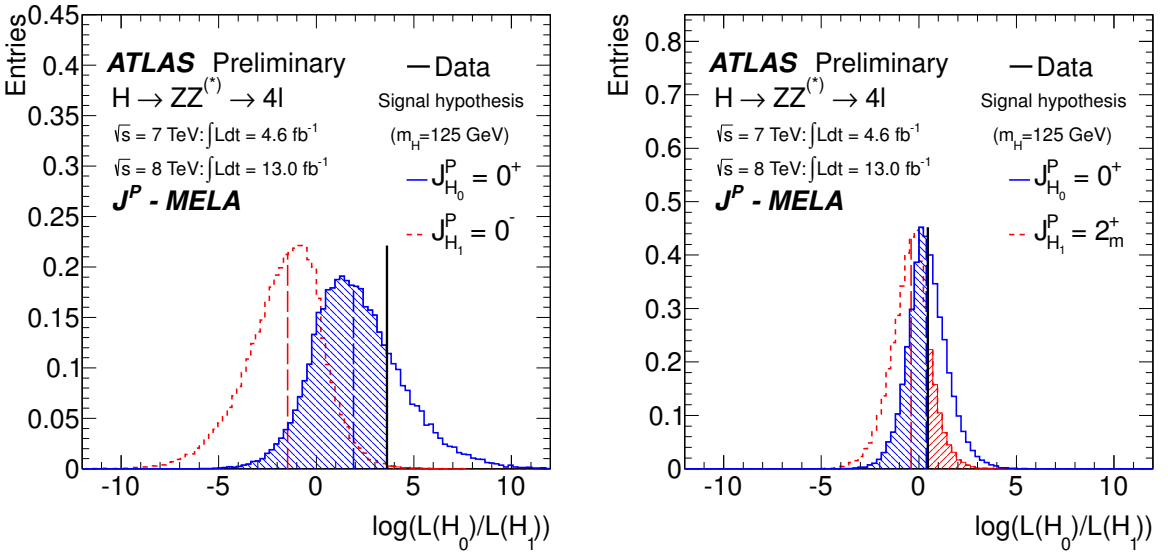

Figure 8. Distribution of the likelihood ratio of 50k pseudo-experiments in the $H \to ZZ^{(*)} \to 4\ell$ channel, corresponding to the spin 0^+ and spin 0^- hypotheses (left) and to the spin 0^+ and spin 2^+ hypotheses [5].

9. Conclusions

An update of the ATLAS results in the search for the Higgs boson, including an integrated luminosity of 4.6 – 4.8 fb^{-1}of data at $\sqrt{s} = 7$ TeV and 13 fb^{-1}of data at $\sqrt{s} = 8$ TeV was presented. The observation of a new particle compatible with the SM Higgs boson is confirmed in the $H \to \gamma\gamma$ channel alone, as well as in the combination of 5 channels. For the fermionic decays there is not yet sufficient sensitivity for an observation, although results are fully consistent with the signal plus background hypothesis. The bosonic decays are used to make first measurements of the mass, spin and parity of the candidate boson.

The combined signal strength from all 5 channels is $\mu = 1.35 \pm 0.19(\text{stat.}) \pm 0.15(\text{syst.})$,

which is compatible with the SM expectation ($\mu = 1$). The combined mass measurement from the $H \to ZZ^{(*)} \to 4\ell$ and $H \to \gamma\gamma$ channels is $125.2 \pm 0.3(\text{stat.}) \pm 0.6(\text{syst.})$ GeV.

Using $H \to ZZ^{(*)} \to 4\ell$ and $H \to \gamma\gamma$ events, various spin hypotheses ($0^{\pm}$ and $2^{\pm}$) are tested. In all cases, the SM hypothesis (0^{+}) is favored by the observation.

References

[1] ATLAS Collaboration 2008 *JINST* **3** 8003
[2] CMS Collaboration 2008 *JINST* **3** 8004
[3] ATLAS Collaboration 2012 *Physics Letters B*
[4] CMS Collaboration 2012 *Physics Letters B*
[5] ATLAS Collaboration 2012 *ATLAS-CONF-2012-169* URL `http://cds.cern.ch/record/1499628`
[6] ATLAS Collaboration 2012 *ATLAS-CONF-2012-168* URL `http://cds.cern.ch/record/1499625`
[7] ATLAS Collaboration 2012 *ATLAS-CONF-2012-158* URL `http://cds.cern.ch/record/1493601`
[8] ATLAS Collaboration 2012 *ATLAS-CONF-2012-160* URL `http://cds.cern.ch/record/1493624`
[9] ATLAS Collaboration 2012 *ATLAS-CONF-2012-161* URL `http://cds.cern.ch/record/1493625`
[10] ATLAS Collaboration 2012 *ATLAS-CONF-2012-170* URL `http://cds.cern.ch/record/1499629`